MILLISECOND PYROLYSIS — MATHEMATIC MODEL AND PARAMETRIC SENSITIVITY

Zina VALÁŠKOVÁ and Josef HORÁK

Department of Organic Technology,
Prague Institute of Chemical Technology, 166 28 Prague 6

Received July 5, 1988
Accepted September 20, 1988

Ethane–water vapour pyrolysis and the influence of the system parameters on the pyrolysis furnace behaviour were studied using mathematical model describing the reactor constructed from Field's pipes. The parameters under discussion are following: reaction mixture feed rate, inlet pressure, heat transferrer temperature (furnace temperature), addition of overheated water vapour, thickness of coke layer on the reactor walls and radiation heat transfer inside the reactor. All parameters were found to be important. For feed rate, furnace temperature and ethane–water ratio an optimum values set can be evaluated. Coke formation on the reactor walls in case the coke layer is very thin can improve the heat transfer due to surface emissivity increasing. Otherwise the coke layer effect is negative.

The pyrolysis reactor is constructed from Field's pipes (tube in tube elements) 10 m in length. Due to the used construction elements two different reaction spaces exist: the space between the two pipes is called annular reactor, the space inside the internal tube is called internal reactor. The reaction mixture flows inside by the annular space, then the flow direction is turned about (at the turning space) and the mixture flows outside by the internal reactor tube. More than thirty reactor elements are placed into the combustion chamber, where the combustion products (the heat supplier) flow. The combustion chamber is supposed to be ideally mixed. See Fig. 1 for the scheme of the furnace and spaces.

On carrying the pyrolysis out it is necessary to follow the tubes skin temperatures along the whole reactor, reaction mixture output temperature, pressure drop, ethylene, propylene and butadiene yields and energy consumption for 1 kg ethylene production or 1 kg ethane transformation.

THEORETICAL

The model consists of two parts — the combustion chamber and the reactor space. In the former one either zonal method or a simplified method can be used for the chamber simulation. In the latter part all processes inside the reactor tubes are simulated. The boundary between the two spaces is formed by the outside wall of

the reactor, the temperature of which is the only spaces connection. Consequently, both spaces can be simulated separately with the boundary temperature iterations.

The reactor itself is divided into two parts – the outside (annular) reactor and the internal reactor with the boundary formed by the outside wall of the internal reactor tube. With prediction of this boundary temperature profile it is possible to simulate the reactor parts in sequence, the iterations of the boundary temperature profile necessarily occur.

Mathematical Model of the Reactor Space

See Fig. 2 for denotation of the quantities. Then the following heat balances must hold:

$$\frac{\mathrm{d}Q}{\mathrm{d}z} = \frac{\mathrm{d}Q_{c1}}{\mathrm{d}z} + \frac{\mathrm{d}Q_r}{\mathrm{d}z} \tag{1a}$$

$$(T_1 - T_3)/A_1 = A_2(T_3 - T_4) + A_3[(T_3/100)^4 - (T_5/100)^4] \tag{1}$$

$$\frac{\mathrm{d}Q_{c2}}{\mathrm{d}z} + \frac{\mathrm{d}Q_r}{\mathrm{d}z} = \frac{\mathrm{d}Q_{c3}}{\mathrm{d}z} \tag{2a}$$

$$A_4(T_4 - T_5) + A_3[(T_3/100)^4 - (T_5/100)^4] = A_6(T_8 - T_9) \tag{2}$$

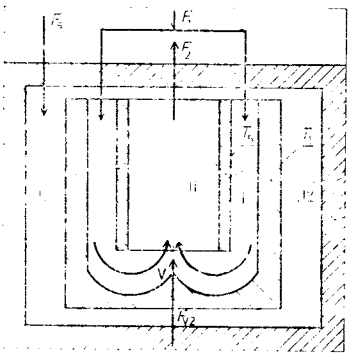

FIG. 1

Scheme of the furnace. I, II reactor spaces: I annular reactor, II internal reactor; III combustion chamber; IV furnace walling; V turning space; T_1, T_5 boundary temperature profiles

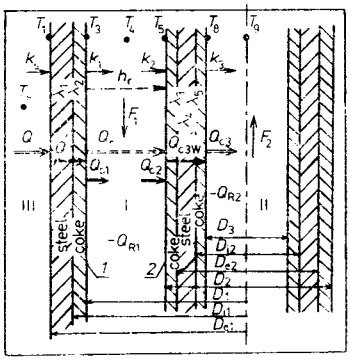

FIG. 2

Scheme of the heat flows and quantity marking in a single zone. I Annular reactor, II internal reactor, III combustion chamber; *1*, *2* annular reactor walls surfaces

$$\frac{dQ_{c3}}{dz} = \frac{dQ_{c3w}}{dz} \tag{3a}$$

$$(T_5 - T_8)/A_5 = A_6(T_8 - T_9)\,. \tag{3}$$

The parameters A_1 to A_6 are defined as follows:

$$A_1 = [\ln(D_{e1}/D_{i1})/\lambda_1 + \ln(D_{i1}/D_1)/\lambda_2]/(2\pi) \tag{4a}$$

$$A_2 = k_1 D_1 \pi \tag{4b}$$

$$A_3 = h_r D_2 \pi\,, \tag{4c}$$

where

$$h_r = \varphi_{1,2}\,.\,5{\cdot}67\Big/\left[\frac{1}{\varepsilon_2} + S_2\left(\frac{1}{\varepsilon_1} - 1\right)\Big/S_1\right] \tag{4d}$$

$$A_4 = k_2 D_2 \pi \tag{4e}$$

$$A_5 = [\ln(D_2/D_{e2})/\lambda_3 + \ln(D_{e2}/D_{i2})/\lambda_4 + \ln(D_{i2}/D_3)/\lambda_5]/(2\pi) \tag{4f}$$

$$A_6 = k_3 D_3 \pi\,. \tag{4g}$$

For the reaction mixture temperature in the annular reactor holds:

$$\frac{dT_4}{dz} = [A_2(T_3 - T_4) - A_4(T_4 - T_5) - Q_{R1}]/(F_1 c_{p1})\,. \tag{5}$$

For the reaction temperature in the internal reactor holds:

$$\frac{dT_9}{dz} = [A_6(T_8 - T_9) - Q_{R2}]/(F_2 c_{p2})\,. \tag{6}$$

For the heat transfer from the combustion chamber to the reactor holds:

$$\frac{dQ}{dz} = A_2(T_3 - T_4) + A_4[(T_3/100)^4 - (T_5/100)^4]\,. \tag{7}$$

For the heat transfer into the internal reactor holds:

$$\frac{dQ_{c3}}{dz} = A_6(T_8 - T_9)\,. \tag{8}$$

Through the Eqs (7) and (8) the reactor heat suply can be traced.

For the pressure drop holds:

$$\frac{dP}{dz} = -3{\cdot}242 \,.\, 10^{-3} \,.\, F^2 f RT/(P \,.\, 10^6 \,.\, MD^4 D_{eq}) \tag{9}$$

$$f = 0{\cdot}0014 + 0{\cdot}125/Re^{0{\cdot}32} \,. \tag{10}$$

For the residence time holds:

$$\frac{dt}{dz} = \pi D^2 MP \,.\, 10^3/(4FRT) \,. \tag{11}$$

In Eqs (*9*) and (*11*) for the annular reactor $F = F_1$, $T = T_4$, $P = P_1$, $D^4 = (D_1^2 - D_2^2)^2$, $D_{eq} = D_1 - D_2$; for the internal reactor $F = F_2$, $T = T_9$, $P = P_2$, $D = D_{eq} = D_3$.

Mass balances for reaction components can be written as a set of equations in the form (in dependence on the used reaction kinetics system because this kinetics part of the modular program can be changed according to the input reaction mixture composition):

$$\frac{dc_I}{dz} = \pi D_{eq}/(4F) \,.\, \sum_I r_I n_{i,I} \,, \tag{12}$$

the shape of the reaction rate r_I depends on used kinetics description.

For the reaction heat holds:

$$\frac{dQ_R}{dz} = \pi D_{eq}^2/4 \,.\, \sum_I r_I \, \Delta H_I \tag{13}$$

Program Description and Function

On the base of presented mathematical model a modular computer program was constructed and used for the simulation of ethane pyrolysis reactions in the reactor of tube in tube type with a very short residence time.

The necessary input data for the computer program are following: data describing the reactor and furnace geometric arrangement; reaction mixture input temperature, pressure, feed rate and composition; data for combustion chamber simulation by zonal method and combustion products temperature; estimate of boundary temperature profile inside the reactor.

As a result of mathematic simulations the following output data can be obtained: the profiles of temperatures, concentrations and pressure along both parts of the reactor; reaction mixture residence time; required power of the furnace, power input of the reactor and heating gas feed rate.

Independent part of the program is formed by physical properties data-bank, program for reaction kinetics description and modular block for the control of the technological iterations. These parts can be modified according to the user's demands. When solving technological tasks, e.g. searching an optimal load of the reactor for desired output degree of conversion, searching the tubes diameters for which the skin temperature profile is equal to the highest permissible one, ... the concrete logical control conditions and demands must be added to the iteration controlling block.

Iterations of the Temperature Profiles

The computation of the tube in tube type reactor is complicated by the internal coupling between the internal and annular reactor (spaces II and I – Fig. 1). A direct interaction occurs there only through the temperature of the reaction mixture; the heat exchange between the two spaces depends on their temperatures. Besides, an influence of concentrations and pressure changes occur, but these interactions are active only in the direction of the reaction mixture flow and do not increase the amount of necessary iterations.

On searching the correct temperature profiles from the heat balances, we took advantage of experience in modelling heavy endothermic processes[1-3] which have damping effects and lead to the system of autocorrelation functions. That is why the method of repeated computation was used for the inside boundary temperature profile iterations when the interactive term value equals to the value from the previous iteration. The problem of iterations occurs only on simulating the annular reactor. On integrating the internal reactor space the problem falls off as the value of the interactive term can be calculated from the results of annular space integration.

The problem of iterations is then concentrated on determining the spaces boundary skin temperatures.

Description of the Combustion Chamber

The program allows using two methods for the combustion space simulation.

Method A: This method comes from the zonal method[4]. It is assumed that the volume zone is ideally mixed, the outer reactor surface and the furnace walling are of Lambert's type and grey, the combustion products were approximated by 1 + 3 model (one diathermic and three grey gases).

Method B: During previous simulations and experimental verifications it was proved that the combustion chamber can be taken as an ideally mixed space with constant temperature of combustion products while the furnace walling temperature changes only slightly according to the changes of heat flow to the reaction space.

Thus the changes of the radiation zones structure are small. These facts enable to simplify the combustion chamber modelling. During the first furnace iteration in the first integration step the radiation heat transfer coefficient is calculated using the results gained from the zonal method. It is assumed that the coefficient is independent on the tube wall temperature. During next integration steps the radiation heat transfer coefficient is used instead of the zonal method.

The simplification was accepted due to the following facts: As there is an uncertainty in the emissivity of the tube wall and the furnace walling, the radiation heat exchange is uncertain, too; the rate of heat transfer from the combustion products to the reactor is influenced especially by the "hot side" of the transfer, the reactor skin temperature influence is only slight because of the difference in the fourth powers ($T_s^4 \gg T_1^4$).

System of Operation During the Furnace Simulation

The length of the reactor is divided into several zones – integration steps. The physical properties and temperatures of the tubes surfaces are assumed to be constant in a single zone. The combustion products temperature is supposed to be constant along the whole furnace.

The program operates in the following steps:

1. Computation of the annular reactor: Computer reads the given input data (reaction mixture temperature, pressure and composition) and estimates of boundary skin temperatures T_1 and T_5. By numerical solution of Eqs (*1*), (*5*), (*7*), (*9*)–(*13*) we get the reaction mixture temperature, pressure and composition (the input values for the next zone), residence time, tube wall temperature T_3 and heat supply Q for the zone.

2. Combustion chamber simulation: One of the two methods is used and the reactor skin temperature T_1 is evaluated from the required heat supply Q. If the estimated and computed values of temperature T_1 are the same, the next zone is integrated; if not – a new estimate of the skin temperature T_1 is made and the same zone is calculated from its beginning

3. Turning space. After the whole annular reactor simulation, the turning space is calculated. The reactor construction enables to add some amount of overheated water vapour to the reaction mixture to increase the reaction temperature in the internal reactor space. If any water vapour is added, the new concentrations, temperature and pressure are evaluated; if not, the output values of the annular reactor are taken as the input values to the internal reactor.

4. Integration of the internal reactor. From known temperatures T_3, T_4 and input value T_9 the new values of temperatures T_5 and T_8 are setted solving Eqs (*2*) and (*3*). Then the set of Eqs (*6*), (*8*)–(*13*) is solved for each zone.

5. Computation accuracy testing. After the whole internal reactor has been calculated, the estimated and computed values of boundary temperature profile T_5 are compared. If there are differences greater than the required accuracy, the calculated values T_5 are taken as new estimates and the furnace is simulated from the beginning. If there are no differences, the furnace simulation is ended and the heat supply to the whole furnace and the heated gas feed rate are calculated.

6. Technological iterations. If there is no technological iteration required, the simulation ends with printing. On the other hand the simulation control is trasnferred to the technological iteration controlling block and controlling conditions and demands are tested. If they are not fulfilled the furnace inputs are changed and new furnace simulation occurs.

CALCULATIONS

To ilustrate the program possibilities and the system behaviour and parametric sensitivity the ethane–water vapour pyrolysis was studied. The used kinetics scheme and the reaction rate equations are presented in Table I, the basic system parameters are the following: reaction mixture input pressure 0·3 MPa, input temperature 854 K; input feed rate of ethane $F_B = 0{\cdot}071$ kg s^{-1}, of water vapour $F_V = 0{\cdot}076$ kg . . s^{-1}; combustion products temperature $T_s = 1\,390$ K, parameter $A_3 = 0{\cdot}495$, annular reactor space walls emissivity $\varepsilon_1 = \varepsilon_2 = 0{\cdot}6$, none coke sediment on the reactor walls. Reactor tubes diameters: $D_{i1} = 0{\cdot}082$ m, $D_{e1} = 0{\cdot}102$ m, $D_{i2} = 0{\cdot}05$ m, $D_{e2} = 0{\cdot}06$ m. Reaction mixture feed rate in the annular reactor $F_1 = F_V + F_B$, in the internal reactor $F_2 = F_1 + F_{V2}$.

RESULTS AND DISCUSSION

Influence of Combustion Chamber Simulation Method

The influence of the used method for the combustion chamber simulation on the furnace behaviour is illustrated on Figs 3 and 4. The profiles of temperatures, concentrations and pressure along the reactor are nearly the same; small differences (to 3 K) occur only on temperatures profiles T_1 and T_3. Thus using the simplified method *B* for combustion chamber simulation seems to be quite correct for this case. The computation time is more than twice shorter.

Regime Characteristics Determination

As the system parameters were found to change only the curves position and not their shape, some important points were chosen to illustrate the influence of the parameter changes. The points under discussion are following: minimum and ma-

ximum reactor skin temperature T_1, minimum and maximum border (internal reactor tube skin) temperature T_5, reaction mixture output temperature T_9, temperature of the reaction mixture at the turning space – i.e. maximum reaction mixture temperature in the annular reactor – T_{4max} (the temperature points are marked on Fig. 3), output concentration of ethane and ethylene and ethylene concentration at the turning space (these points are marked on Fig. 4).

Reaction Mixture Feed Rate Influence

Reaction mixture feed rate has a great influence on the system behaviour as it can affect not only the residence time of the reaction mixture but even the heat transfer, temperatures, heat consumption, conversions of reaction components etc. Figs 5 and 6 illustrate the influence of the feed rate change on the concentrations, pressure and temperatures profiles along both parts of the reactor.

The higher the feed rate, the lower are the values of all temperatures (Fig. 7*a*), the reaction mixture residence time (Fig. 8*c*) and exit pressure (Fig. 8*a*). If a technological value of the output pressure is to be kept, the input pressure must be increased

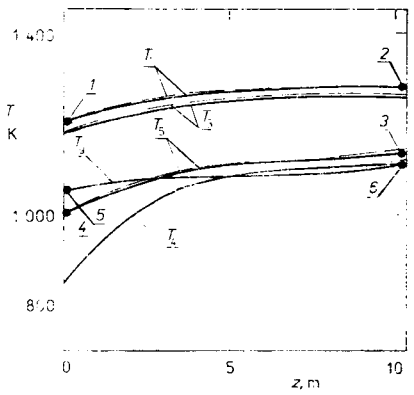

FIG. 3

Influence of method for combustion chamber simulation on temperature profiles along the reactor. Basic conditions; ——— simplified method; — — — zonal method; ● minimum and maximum traced values on the temperatures profiles: *1* T_1 minimum, *2* T_1 maximum, *3* T_5 maximum, *4* T_5 minimum, *5* T_9 output, *6* T_4 at the turning space

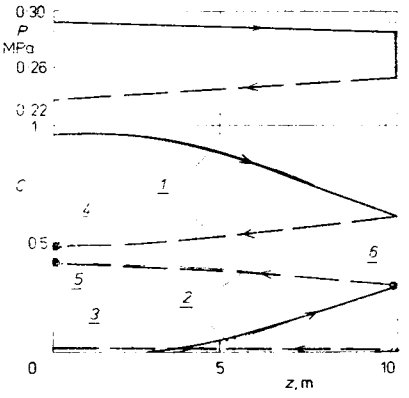

FIG. 4

Influence of method for combustion chamber simulation on pressure and concentration profiles along the reactor. Basic conditions; ——— zonal method; ——— simplified method; *1* ethane, *2* ethylene, *3* butadien, propylene; ——— annular reactor, — — — internal reactor, —→— flow direction; ● traced points: *4* ethane, *5* ethylene output concentration; *6* ethylene concentration at the turning space

together with increasing feed rate. The increasing pressure further affects the furnace behaviour as discussed in the next section.

With rising feed rate an increase of the heat transfer coefficients in the annular reactor space can be observed (Fig. 8*b*) and the driving force of the heat transfer from the combustion chamber to the reactor wall also increases due to decreasing skin temperature T_1. Consequently the heat flux from combustion products to the reaction mixture increases while the heat flow to the internal space passes the maximum (Fig. 9*a*).

These changes simultaneously with decreasing reaction temperature and reaction mixture residence time influence the concentrations of reaction components. The ethylene concentration at both turning space and reactor output passes maximum (Fig. 7*b*), which means that an optimum value of the feed rate must exist. Consequently a minimum of the heat consumption for production of 1 kg ethylene (or for 1 kg ethane transformation) exists (Fig. 9*b*).

Under a very low feed rate the reaction temperature is so high that the side reactions can occur so as the concentration of ethylene decreases along the internal reactor (Fig. 5 – thin line 2) and the output ethylene concentration is lower than the concentration at the turning space (Fig. 7*b* – hatched area). Such region of low feed rate and high reaction temperature is unsuitable for industrial pyrolysis.

TABLE I

Ethane pyrolysis kinetics

Chemical reaction	Reaction rate r_I[a] kmol m^{-3} s^{-1}	Reaction number I
$CH_3—CH_3 \rightleftharpoons CH_2=CH_2 + H_2$	$r_1 = K_1(c_1 - c_2c_3/K_{e1})$	1
$CH_3—CH_3 \rightleftharpoons 1/2\,CH_4 +$ $+ 1/2\,CH_3—CH_2—CH_3$	$r_2 = K_2c_1[1 - c_4c_6/(c_1^2K_{e2})]$	2
$CH_3—CH_2—CH_3 \rightleftharpoons CH_3—CH=CH_2 + H_2$	$r_3 = K_3(c_6 - c_5c_3/K_{e3})$	3
$CH_3—CH_2—CH_3 \rightarrow CH_4 + CH_2=CH_2$	$r_4 = K_4c_6$	4
$CH_3—CH=CH_2 \rightleftharpoons CH\equiv CH + CH_4$	$r_5 = K_5(c_5 - c_7c_4/K_{e5})$	5
$CH_2=CH_2 + CH\equiv CH \rightarrow$ $\rightarrow CH_2=CH—CH=CH_2$	$r_6 = K_6c_7c_2$	6
$CH_2=CH_2 \rightarrow CH\equiv CH + H_2$	$r_7 = K_7c_2$	7
$CH_3—CH_3 + CH_2=CH_2 \rightarrow$ $\rightarrow CH_4 + CH_3—CH=CH_2$	$r_8 = K_8c_1c_2$	8
$CH_3—CH_3 \rightarrow 1/2\,CH_2=CH_2 + CH_4$	$r_9 = K_9c_1$	9

[a] E activation energy; c_i reaction mixture component concentration, kmol m^{-3}: 1 ethane, 2 ethylene, 3 hydrogen, 4 methane, 5 propylene, 6 propane, 7 acetylene, 8 butadiene, 9 water

Hydrocarbon Mixture to Water Vapour Ratio Influence

The pyrolysis hydrocarbon reaction mixture (F_B) is diluted with water vapour (F_V). The value of the dilution is important for the system behaviour. With decreasing dilution ratio $F_V : F_B$ the temperatures are lower, the reaction mixture residence time is longer and the output ethylene concentration decreases. Consequently the heat consumption for 1 kg ethylene production decreases, too. (These aspects are illustrated on Figs 7, 8, 9 with black points.)

Mathematic simulation proved that an optimum combination of reation mixture feed rate and dilution ratio exists but the position of the optimum depends on the hydrocarbon mixture composition and the reactor tubes geometry.

Reaction Mixture Input Pressure Influence

With rising input pressure of reaction mixture, the pressure drop along the reactor decreases (Fig. 10*a*). Consequently the heat transfer coefficient to the annular reactor space decreases (Fig. 10*b*) and, simultaneously with the residence time increasing (Fig. 10*d*), the reaction mixture output temperature rises while the temperature at the turning space decreases (Fig. 10*f*). These changes as well as the negative pressure effect on the process selectivity cause the drop of ethylene output concentration

TABLE I
(*Continued*)

Rate constant $K_I = A_I \cdot \exp(-E_I/RT)$		Equilibrium constant K_{cI}	ΔH_I J mol^{-1}
$A_I \cdot 10^{-11}$	E_I, J mol^{-1}		
465·2	272 786·3	$5{\cdot}348 \cdot 10^4 \cdot \exp(-136\,309{\cdot}5/RT)$	137 076
38·5	272 995·5	1·5	−4 668·3
0·5888	214 589·1	$6{\cdot}4925 \cdot 10^4 \cdot \exp(-119\,222{\cdot}7/RT)$	124 348
1·4076	211 702·2	—	81 349·5
3·794	248 478·2	$1{\cdot}91 \cdot 10^4 \cdot \exp(-126\,184{\cdot}6/RT)$	131 549
10·26	172 625·2	—	−116 895
400·	300 000	—	174 548
708·3	252 829·4	—	22 064·4
30·	280 317·2	—	36 006·5

(Data were gained from VÚCHZ Brno.)

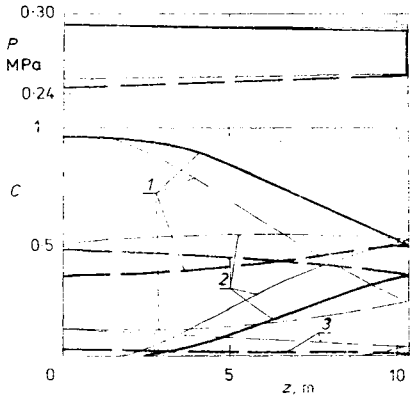

FIG. 5

Influence of reaction mixture feed rate on the concentrations and pressure profiles along the reactor tubes. Basic conditions; $F_V : F_B = 1{\cdot}07$; $F_1 = 0{\cdot}1$ kg s^{-1} ———; $F_1 = 0{\cdot}066$ kg s^{-1} ———; ——— annular reactor, – – – internal reactor, *1* ethane, *2* ethylene, *3* butadiene, propylene, methane

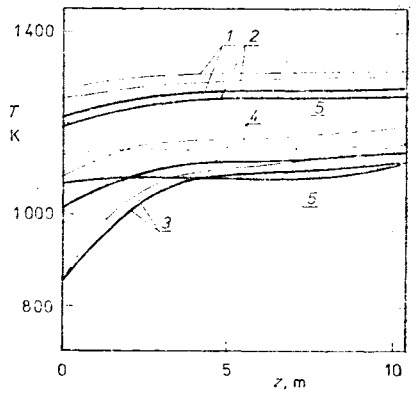

FIG. 6

Influence of reaction mixture feed rate on the temperature profiles along the reactor tubes. Basic conditions, $F_V : F_B = 1{\cdot}07$; ——— $F_1 = 0{\cdot}1$ kg s^{-1}; – – – $F_1 = 0{\cdot}066$ kg s^{-1}; temperatures: *1* T_1, *2* T_3, *3* T_4, *4* T_5, *5* T_9

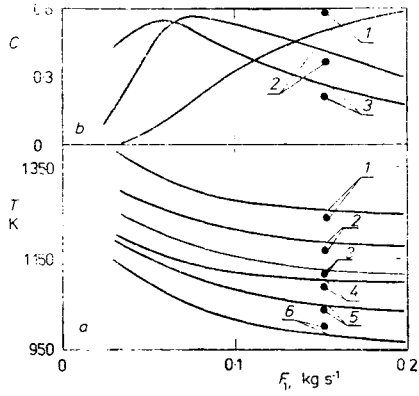

FIG. 7

Influence of the reaction mixture feed rate on the temperature profiles (*a*) and reaction mixture composition (*b*). Basic conditions; $F_V : F_B = 1{\cdot}07$; ● $F_V : F_B = 0{\cdot}5$; *a* temperatures: *1* T_1 max, *2* T_1 min, *3* T_5 max, *4* T_4 at turning space, *5* T_9 output, *6* T_5 min; *b* concentrations: output of *1* ethane, *2* ethylene; *3* ethylene at turning space; ||||| unsuitable area

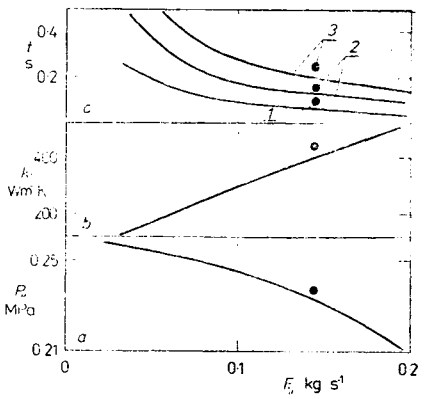

FIG. 8

Influence of reaction mixture feed rate on *a* reaction mixture output pressure, *b* heat transfer coefficient from the tube wall to the annular space (at 1/3 of the tube length), *c* the residence time: *1* at the internal reactor, *2* at the annular reactor, *3* total residence time. Basic conditions; ——— $F_V : F_B = 1{\cdot}07$; ● $F_V : F_B = 0{\cdot}5$

(Fig. 10e). Under further pressure increase, the side reactions are preferred and the output concentration of ethylene still decreases even below the ethylene concentration at the turning space (hatched area on Fig. 10e) while the output concentrations of methane, butadiene and propylene rise. The shape of the concentration profiles for input pressure about 0·65 MPa and feed rate $F_1 = 0{\cdot}147\ \mathrm{kg\ s^{-1}}$ is quite similar to that for the low feed rate (Fig. 5 – thin lines). Fig. 10c illustrates the amount of heat consumption for 1 kg ethylene production and for 1 kg ethane transformation.

It can be concluded by saying the reaction mixture input pressure increase unfavourably affects the system behaviour.

Combustion Products Temperature Influence

As the pyrolysis is an endothermal process, the reactor must be heated with combustion products, the temperature of which is supposed to be constant at the whole

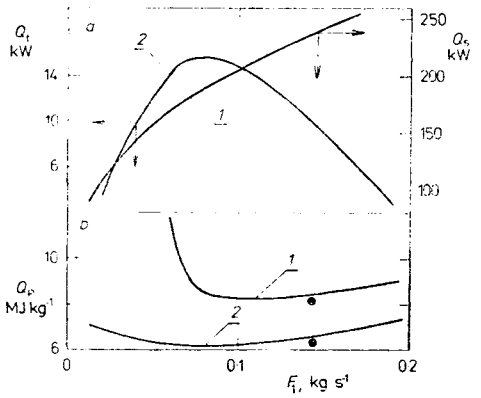

FIG. 9

Influence of reaction mixture feed rate on the heat flows (*a*) and heat consumption (*b*). *a* Heat flow: *1* from the combustion products to the reactor; *2* to the internal reactor. *b* Heat consumption: *1* for 1 kg ethylene production, *2* for 1 kg ethane transformation. Basic conditions; $F_V : F_B = 1{\cdot}07$ ——; $F_V : F_B = 0{\cdot}5$ ●

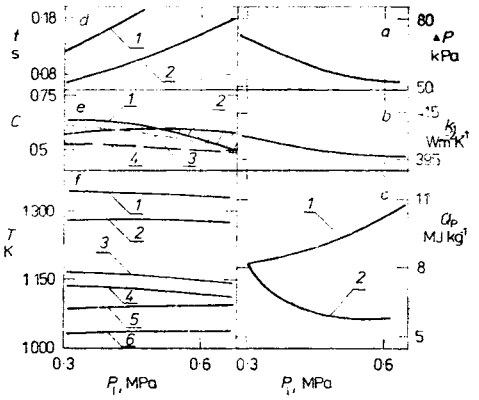

FIG. 10

Influence of the reaction mixture input pressure on *a* pressure drop, *b* heat transfer coefficient, *c* heat consumption for: *1* production of 1 kg ethylene, *2* transformation of 1 kg ethane, *d* reaction mixture residence time at: *1* the annular reactor, *2* the internal reactor, *e* concentration: *1* ethylene output, *2* ethylene at turning space, *3* ethane at turning space, *4* ethane output, *f* temperatures: *1* T_1 max, *2* T_1 min, *3* T_5 max, *4* T_4 at turning space, *5* T_9 output, *6* T_5 min

furnace. The higher the combustion products temperature, the bigger is the driving force of the heat transfer from the combustion chamber to the reactor and the higher are all values of traced temperatures (Fig. 11*a*). Up to certain value of reaction temperature the output concentration of ethylene is influenced favourably but for the reaction temperature above 1 140 K the side reactions are preferred. Consequently the ethylene concentration at the reactor output decreases even under the value at the turning space. This area of high combustion products temperature is then unfavourable (Fig. 11*b*). For the combustion products temperature 1 570 K and feed rate $F_1 = 0{\cdot}147\ \mathrm{kg\ s^{-1}}$ the concentration profiles are nearly the same as for the low feed rate (Fig. 5). The course of the temperature profiles is presented on Fig. 12 (compare with Fig. 3). In this case the skin temperature of the reactor is so high that such regime can be even dangerous for the reactor tubes material.

Simultaneously, an energy optimum for 1 kg ethylene production or ethane transformation must exist (Fig. 11e) as, in consequence of the temperature changes, the

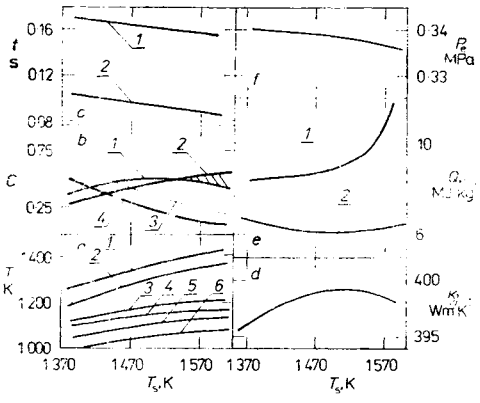

FIG. 11

Influence of the combustion products temperature on *a* temperature profiles: *1* T_1 max, *2* T_1 min, *3* T_5 max, *4* T_4 at turning space, *5* T_9 output, *6* T_5 min; *b* concentrations: *1* ethylene output, *2* ethylene at turning space, *3* ethane at turning space, *4* ethane output; *c* residence time at: *1* annular reactor, *2* internal reactor; *d* heat transfer coefficient; *e* heat consumption for: *1* 1 kg ethylene production, *2* 1 kg ethane transformation; *f* reaction mixture output pressure

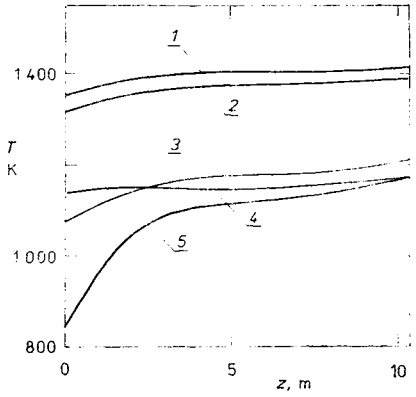

FIG. 12

Influence of combustion products temperature on the temperature profiles. *1* T_1 skin temperature, *2* wall temperature T_3, *3* border wall temperature T_5, *4* reaction temperature T_9, *5* reaction temperature T_4. Basic conditions but $T_s = 1\ 570$ K

residence time of reaction mixture, the heat transfer coefficient to the annular reactor space and the output pressure are changing (Fig. 11c–e).

Overheated Water Vapour Addition Influence

Construction of the reactor enables to add overheated water vapour to the reaction mixture at the turning space. The addition causes skip rise of the reaction temperature at the input to the internal reactor (Fig. 13*a*, lines *5*, *6*). After water vapour addition the feed rate at the internal reactor F_2 is higher and consequently higher is the heat transfer coefficient to the internal reactor k_3 (Fig. 13*c*). However – due to the heat transfer driving force deep decrease – the amount of the heat transferred into the internal reactor is lower (Fig. 13e) and consequently the heat supplied for the reactor from the combustion chamber decreases, too. These facts cause drop of the heat consumption for 1 kg ethylene production (Fig. 13*f*) while the ethylene output concentration is nearly the same. Other system variables, such as output pressure

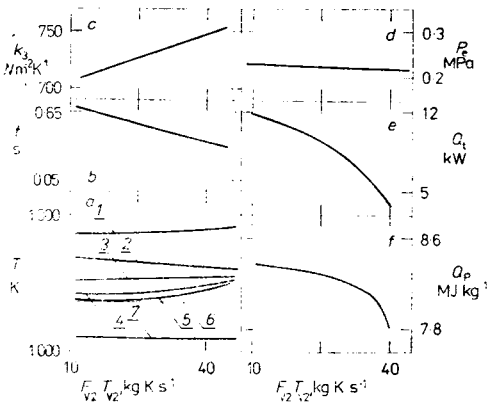

FIG. 13

Influence of water vapour addition on: *a* temperatures: *1* T_1 max, *2* T_1 min, *3* T_9 output, *4* T_5 max, *5* temperature at the input to the internal reactor (after vapour addition), *6* T_4 at the end of the annular reactor (before vapour addition), *7* T_5 min; *b* residence time at the internal reactor; *c* heat transfer coefficient to the internal reactor; *d* reaction mixture output pressure; *e* heat transferred to the internal reactor; *f* heat consumption for 1 kg ethylene production. Basic conditions

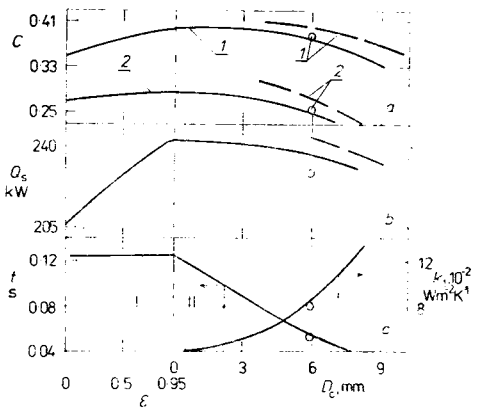

FIG. 14

Influence of tube wall emissivity (I) and coke layer thickness (II) on: *a* ethylene concentration: *1* output concentration, *2* concentration at the turning space (for $D_c \geqq 4$ mm: ——— $D_{c2} = 2$ mm, – – – $D_{c2} = 3$ mm); *b* heat supplied from combustion products to the reactor spaces; *c* residence time at the annular space; convection heat transfer coefficient. Basic conditions; ○ coke layer $D_{c1} = D_{c2} = 3$ mm, none radiation heat transfer at the annular space

and temperatures, change only slightly (Fig. 13). The simulations were carried out for the added water vapour feed rate from 7 to 20% of the reaction mixture feed rate and the vapour temperature was 90 to 190 K higher than that one of the reaction mixture.

Influence of Radiation and Coke Formation Inside the Annular Reactor

Inside the annular reactor the heat can be transferred by two ways: by convection from the tube surfaces to the reaction mixture (heat flows Q_c – Fig. 2) and by radiation from the internal surface of the external reactor tube (surface *1* – Fig. 1) to the external surface of the internal reactor tube (surface 2, heat flow Q_r – Fig. 2). Significance of the radiation depends on the surfaces temperatures, emissivities, reactor geometry, reaction mixture composition etc.

The emissivity of pure steel is said to be about 0·6 while pyrolysis coke emissivity is supposed to be from 0·95 to 0·97 (see ref.[5]). If none radiation heat transfer occurs, the temperature of the tube wall T_5 must be situated between the reaction mixture temperatures T_4 and T_9 in both reaction spaces. The heat can be transferred either from the annular reactor to the internal reactor or by contraries in dependence on the reaction mixture temperatures. If any radiation heat transfer occurs, the border tube wall temperature T_5 becomes higher than the reaction mixture temperatures T_4 and T_9. The length of the reactor tube part where the border temperature T_5 is higher depends on the emissivity of the annular reactor wall surfaces.

The higher the surfaces emissivity and consequently the radiation heat transfer at the annular reactor, the higher is the border wall temperature T_5. The heat can be transferred simultaneously from the border tube wall to both reactor spaces (see Fig. 3 – line T_5). The total heat balance proved that the heat from the combustion chamber is supplied not only to the annular reactor but even to the internal reactor. Due to this fact, the amount of heat transferred to the reaction mixture increases and so do the output reaction temperature and ethylene concentration (Fig. 14*a*, *b*). Consequently the skin temperature of the reactor T_1 slightly decreases. The emissivity influence on temperatures, ethylene concentration and heat supply is illustrated on Figs 14 and 15, part I. A coke layer, the emissivity of which is about 0·95 while its thickness is stil negligible, can be formed during the few first hours of pyrolysis course[5]. The favourable emissivity increase influence on the system behaviour is interesting theoretically but due to the coke formation cannot be utilized to improve the industrial reactors regime.

During the pyrolysis course the thickness of coke layer is increasing on both internal wall of external reactor tube and external wall of internal reactor tube. The coking proceeds more slowly on the surface 2 due to lower temperature T_5 than T_3. Due to coke formation, the heat transfer coefficients through the tube wall decrease. But along with that – in consequence of annular reactor effective section

decreasing and flow rate increasing – the heat transfer coefficient from the annular space wall to the reaction mixture significantly rises (Fig. 14*c*). Simultaneously other changes occur: the maxima of skin temperature T_1 and border temperature T_5 increase while minima of them decrease; the reaction temperature at the annular reactor slightly increases but the output temperature decreases (Fig. 15*a*). Due to those temperature profiles changes both the heat supply from the combustion chamber and ethylene output concentration stay at nearly constant levels for some period and then rapidly drop (Fig. 14*a*, *b*). It is caused by the fact that the rising flow rate compensates to a considerable degree the coke insulating effect.

With rising coke layer thickness the reaction mixture output pressure significantly decreases (Fig. 15*b*). If a technological value is to be kept, the input pressure must be increased. However, the pressure increase farther strengthens the negative influence of coke formation.

The simulation proved that the state, in which the coke layer on the surface *2* is thicker than that one on the surface *1*, is favourable for the output ethylne concentration (Fig. 14*a*, – – – lines). The insulating coke layer prevents the heat transfer into the internal reactor, the reaction temperature T_4 at the annular reactor

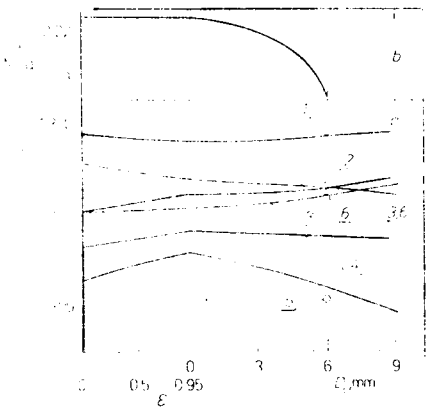

FIG. 15

Influence of tube wall emissivity (I) and coke layer thickness (II) on temperatures (*a*) and reaction mixture output pressure (*b*). Basic conditions; $D_c = D_{c1} + D_{c2}$; *1* T_1 max, *2* T_1 min, *3* T_4 at the turning space, *4* T_9 output, *5* T_5 min, *6* T_5 max; —— radiation heat transfer at annular space occurs; o none radiation heat transfer at annular space

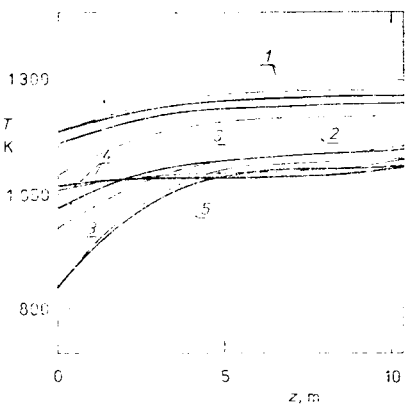

FIG. 16

Influence of coke layer on temperature profiles course along the reactor. Basic conditions; $D_{c1} = 3$ mm, $D_{c2} = D_{c3} = 1$ mm of coke – – –; none coke ——— ($D_{c1} = D_{c2} = D_{c3} = 0$). *1* Skin temperature T_1, *2* wall temperature T_3, *3* border wall temperature T_5, *4* reaction temperature T_9 at internal reactor, *5* reaction temperature T_4 at annular reactor

is higher and consequently the output ethylene concentration increases. In practice such state cannot be reached (maybe after imperfect coke removing).

Changes in the temperature profiles courses due to coke formation are illustrated on Fig. 16. On Figs 14 and 15 the state with coke layers on the tube walls but without radiation heat transfer inside the annular reactor is illustrated. The reactor skin temperature is nearly the same as in the case with radiation but the reaction temperature is lower along the whole reactor and the output concentration of ethylene is lower, too (Figs 14 and 15, ○ points).

The coke formation was proved to be very important for carrying the pyrolysis out, especially in the reactor constructed from the pipe in pipe elements, where the diameters of reactor spaces are small.

CONCLUSION

The constructed modular program was proved to be able to simulate the millisecond pyrolysis reactor behaviour and the system sensitivity. The sensitivity to the system parameters changes is not negligible at all. The main role is played not only by the reaction mixture feed rate and the coke formation, but also by the water vapour reaction mixture dilution and by the reactor geometry which can significantly influence the heat transfer to the reaction mixture.

LIST OF SYMBOLS

$A_i - A_5$	system parameters
C	mass fraction of reaction mixture component (without water)
c_i	concentration of reaction component number i, kmol kg^{-1}
c_{p1}, c_{p2}	heat capacity of reaction mixture in space I, II, J kg^{-1} K^{-1}
D_c	general coke layer inside the annular reactor, mm
D_{c1}	coke layer on the surface 1 (Fig. 2), mm
D_{c2}	coke layer on the surface 2 (Fig. 2), mm
D_{c3}	coke layer on the internal surface of the internal reactor tube, mm
D_{e1}, D_{e2}	outer diameter of external resp. internal reactor tube, m
D_{eq}	equivalent diameter, m
D_{i1}, D_{i2}	internal diameter of external resp. internal tube, m
D_1, D_2, D_3	effective diameters (Fig. 2), m
F_B, F_V	feed rate of hydrocarbon mixture resp. water vapour, kg s^{-1}
F_s	combustion products feed rate, kg s^{-1}
F_{V2}	added water vapour feed rate, kg s^{-1}
F_1, F_2	feed rate of reaction mixture in space I resp. II, kg s^{-1}
f	friction coefficient
ΔH_I	reaction heat for reaction number I, J mol^{-1}
h_r	coefficient of radiation heat transfer in space I, W m^{-2} K^{-4}
k_s	coefficient of radiation heat transfer to the reactor, W m^{-2} K^{-4}
k_1, k_2, k_3	coefficients of convection heat transfer, W m^{-2} K^{-1}
M	medium molecular mass of reaction mixture, kg kmol^{-1}

$n_{i,n}$	amount of mole of component *i* in reaction number *I*
P, P_1, P_2	reaction mixture pressure in space I resp. II, MPa
P_i	reaction mixture input pressure, MPa
P_e	reaction mixture output pressure, MPa
ΔP	pressure drop, kPa
Q	heat supply to the annular reactor from combustion chamber in a single zone, W
Q_{c1}, Q_{c2}, Q_{c3}, Q_{c3W}	convection heat flows in reactor (Fig. 2), W
Q_P	heat consumption for 1 kg ethylene production or 1 kg ethane transformation, MJ kg^{-1}
Q_R, Q_{R1}, Q_{R2}	reaction heats in space I resp. II, W
Q_r	radiation heat flow in annular reactor, W
Q_s	heat supplied from the combustion chamber to the whole reactor, kW
Q_t	heat supplied to the internal reactor, kW
R	gas constant, J mol^{-1} K^{-1}
Re	Reynold's number
r_I	reaction rate for reaction number *I*, kmol m^{-3} s^{-1}
S_1, S_2	area of surface *1* resp. surface *2*, m^2
T	temperature, K
T_s	combustion products temperature, K
T_{V2}	temperature of water vapour added at the turning space, K
T_1, T_3, T_5, T_8	temperatures of tubes surfaces (Fig. 2), K
T_4, T_9	temperature of reaction mixture in space I resp. II, K
t	time, s
z	length of the reactor tubes, m
ε_1, ε_2	radiant capacity of surfaces *1* resp. *2* in annular space
$\lambda_{1\,2,3,4,5}$	heat carrying capacities (Fig. 2), W m^{-1} K^{-1}

REFERENCES

1. Vašíček E., Veselý P.: Chem. Prum. *33*, 356 (1983).
2. Horák J., Pragrová M., Olejník J.: Chem. Prum. *34*, 584 (1984).
3. Valášková Z., Horák J.: *Presented at 9th International Congress CHISA, August 30 to September 4, 1987, Prague, Czechoslovakia.*
4. Hottel H. C., Sarofim A. F.: *Radiative Transfer.* McGraw-Hill, New York 1967.
5. Bennet M. J., Price J. B.: J. Mater. Sci. *16*, 170 (1981).

Translated by the author (Z. V.).